Molecular Crystals and Liquid Crystals

Publication details, including instructions for authors and subscription information:
http://www.tandfonline.com/loi/gmcl20

Novel Nonsymmetric Trimeric Liquid Crystals Exhibiting Glassy Nematic State at Low Temperatures

Guan-Yeow Yeap [a], Tiang-Chuan Hng [a], Wan Ahmad Kamil Mahmood [a], Ewa Gorecka [b], Daisuke Takeuchi [c] & Kohtaro Osakada [c]

[a] Liquid Crystal Research Laboratory, School of Chemical Sciences, Universiti Sains Malaysia, Penang, Malaysia

[b] Department of Chemistry, Warsaw, Poland

[c] Chemical Resources Laboratory, Tokyo Institute of Technology, Midori-ku, Yokohama, Japan

Version of record first published: 31 Aug 2012.

To cite this article: Guan-Yeow Yeap , Tiang-Chuan Hng , Wan Ahmad Kamil Mahmood , Ewa Gorecka , Daisuke Takeuchi & Kohtaro Osakada (2008): Novel Nonsymmetric Trimeric Liquid Crystals Exhibiting Glassy Nematic State at Low Temperatures, Molecular Crystals and Liquid Crystals, 487:1, 135-152

To link to this article: http://dx.doi.org/10.1080/15421400802198599

Mol. Cryst. Liq. Cryst., Vol. 487, pp. 135–152, 2008

ISSN: 1542-1406 print/1563-5287 online
DOI: 10.1080/15421400802198599

Taylor & Francis
Taylor & Francis Group

Novel Nonsymmetric Trimeric Liquid Crystals Exhibiting Glassy Nematic State at Low Temperatures

Guan-Yeow Yeap[1], Tiang-Chuan Hng[1], Wan Ahmad Kamil Mahmood[1], Ewa Gorecka[2], Daisuke Takeuchi[3], and Kohtaro Osakada[3]

[1]Liquid Crystal Research Laboratory, School of Chemical Sciences, Universiti Sains Malaysia, Penang, Malaysia
[2]Department of Chemistry, Warsaw, Poland
[3]Chemical Resources Laboratory, Tokyo Institute of Technology, Midori-ku, Yokohama, Japan

Series of nonsymmetric 4-ethyl- and 4-fluoroanilinebenzylidene-2′,4′-oxy-bis(4″-halogenoanilinebenzylidene-4‴oxy)alkanes trimers have been synthesized and characterized. Every member in this series possesses either Cl or Br terminal atoms. The molecular structure of these novel trimers is composed of six aromatic rings interconnected via two methylene spacers and three azomethine linking groups. In each molecule, the two identical methylene spacers vary from either C_4H_8 or C_6H_{12}. The trimers exhibit relatively low T_m and T_c (< 160°C). Three of the homologues with ethyl group are glassy nematic liquid crystals with T_g < 15°C. The low transition temperatures are attributed to the branched molecular architecture which leads to steric hindrance and lesser degree of lateral intermolecular attraction. The liquid crystallinity of the intermediary aldehydes is also investigated.

Keywords: glassy nematic liquid crystals, halogen, low transition, nonsymmetric, trimer

INTRODUCTION

A liquid crystalline trimeric molecule consists of three mesogenic fragments which are linked to each other via two flexible spacers [1,2]. Many of these liquid crystal trimers or trimesogens are symmetrical in terms of molecular structure [3]. However, the nonsymmetric trimers have also been reported in which the cholesteryl ester, biphenyl,

Address correspondence to Guan-Yeow Yeap, Liquid Crystal Research Laboratory, School of Chemical Sciences, Universiti Sains Malaysia, Penang, Malaysia. E-mail: gyyeap@usm.my or gyyeap_liqcryst_usm@yahoo.com

and azobenzene served as three mesogenic fragments [4]. The investigation on liquid crystal dimers and trimers is essential as these materials represent the shorter oligomeric members to model for the technologically important semi-flexible main chain liquid crystal polymers [5,6]. The liquid crystal trimers are also different in comparison to the dimeric systems in terms of physical properties, e.g., exhibiting greater magnitude of T_{N1} alternation among odd and even members [1].

Generally, rod-like molecules are highly favourable to induce mesomorphic behavior due to the high shape anisotropy [7–9]. The presence of lateral substituents is known to perturb the orderings in the liquid crystalline phase and in some cases the mesomorphic properties are completely diminished [10]. In order to further explore the effect of molecular branching on the liquid crystalline properties, several researchers have introduced lateral aromatic fragments to the existing calamitic structures. The results thus obtained show that the influence of a lateral aromatic fragment on liquid crystallinity depends on whether the fragment is attached to the inner or outer rings.

In this paper, we report a series of liquid crystal trimers in which the mesogenic cores comprise 4-ethyl- and 4-fluoroanilinebenzylidene-2′,4′-oxy-bis(4″-halogenoaniline benzylidene-4″-oxy)alkanes with three interconnected benzylideneanilines. The chlorinated and brominated benzylideneaniline moieties are linked to the 2,4-dihydroxybenzaldehyde molecule at *ortho* and *para* positions via the flexible spacers. Unlike banana-shaped liquid crystals, these trimers do not have a rigid bent mesogenic core. The trimeric molecules possess higher degree of flexibility at the centre of the structure and not necessarily adopt the bent geometry like the banana-shaped liquid crystals. The asymmetry of the trimers can be ascribed to the third benzylideneaniline core which branched out from the substituted 2,4-dihydroxybenzaldehyde moiety at the centre. The general structure of the trimers is given as follows:

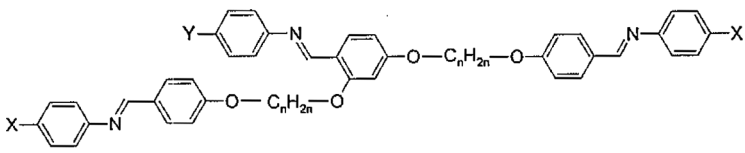

The trimers vary with different combinations of C_nH_2n (where $n = 4$ or 6) methylene spacers, terminal atoms X of Cl or Br and Y of a F atom or C_2H_5, group. The liquid crystalline properties of the homologous compounds are rationalized based upon the molecular geometry, the effect of different halogen atoms and flexibility contributed by the

spacers. The mesomorphic properties of the intermediary aldehydes are also investigated and compared with the title compounds.

EXPERIMENTAL

Synthesis

The synthetic routes are given in Scheme 1. Compounds **1a** and **1b** were synthesized via condensation reaction between 4-hydroxybenzaldehyde and corresponding anilines. Compounds **2a–2d** were obtained via Williamson ether synthesis of **1a** and **1b** with a series of α ω-dibromoalkanes. Compounds **2a–2d** were subsequently reacted with 2,4-dihydroxybenzaldehyde to form the aldehyde-based asymmetric trimers. The intermediary trimers **3a–3d** were then reacted with 4-ethylaniline which also served as a reflux co-medium to give the title compounds **4a–4d**. In a similar manner to 4-ethylaniline, 4-fluoroaniline was also used as co-medium to dissolve **3a–3d** leading to **5a–5d**, respectively. Compounds **3a–3d, 4a–4d**, and **5a–5d** with respective terminal substituents and spacers are listed in Table 1.

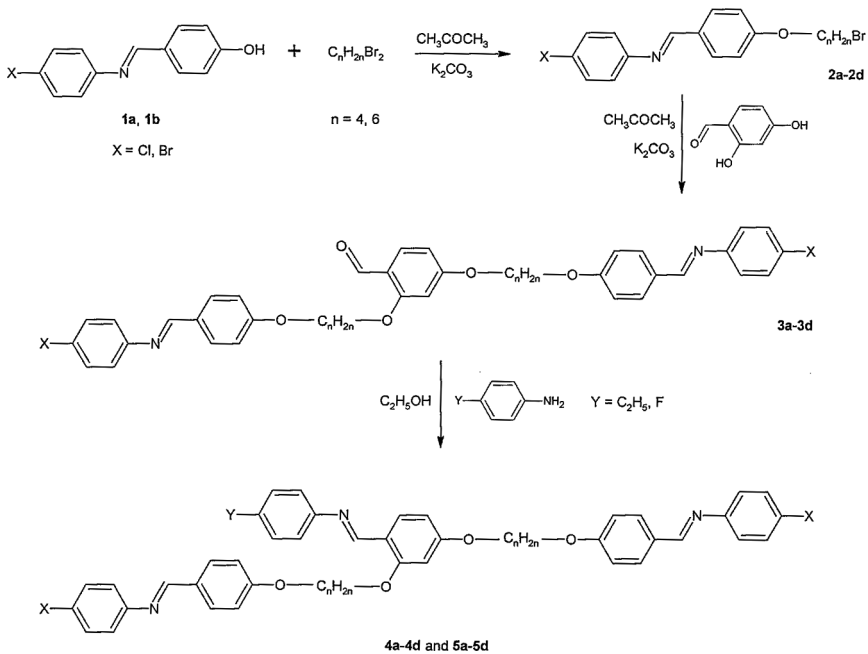

SCHEME 1 The synthetic routes leading to the compounds 4a–4d and 5a–5d.

TABLE 1 List of Intermediary Aldehydes (**3a–3d**) and 4-ethyl- and 4-fluoro Anilinebenzylidene-2′ ,4′-oxy-bis(4″-Halogenoanilinebenzylidene-4‴-oxy)-alkanes Trimers (**4a–4d** and **5a–5d**)

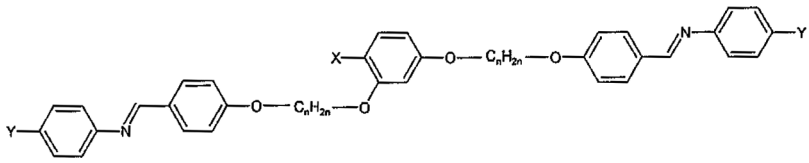

Compound	X	Y	n
3a	CHO	Cl	4
3b	CHO	Cl	6
3c	CHO	Br	4
3d	CHO	Br	6
4a	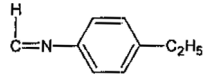	Cl	4
4b	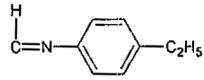	Cl	6
4c	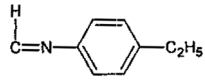	Br	4
4d	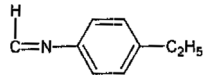	Br	6
5a	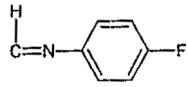	Cl	4
5b	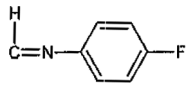	Cl	6
5c	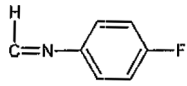	Br	4
5d	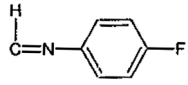	Br	6

Synthesis of Compound 1a

In a round-bottom flask, 4-chloroaniline (3.83 g, 30.0 mmole) in 40 mL absolute ethanol was added to a 50 mL ethanolic solution of 4-hydroxybenzaldehyde (3.66 g, 30.0 mmole). The mixture was heated at 70°C overnight. The resulting solution was left to evaporate off at room temperature whereupon the precipitate was recrystallized from chloroform to yield the pure intermediate. Yield 82%. Elemental analysis: found, C 67.40, H 4.37, N 6.05; calculated ($C_{13}H_{10}NOCI$), C 67.39, H 4.35, N 6.05. IR (KBr) ν/cm^{-1}, 3413 (OH), 1637–1601 (C=N). ^{1}H-NMR ($CDCl_3$) δ/ppm, 5.15 (s, 1H, OH), 6.92 (d, 2H, Ar), 7.14 (d, 2H, Ar), 7.37 (d, 2H, Ar), 7.81 (d, 2H, Ar), 8.37 (s, 1H, CH=N).

Synthesis of Compound 1b

Yield 86%. Elemental analysis: found, C 56.57, H 3.67, N 5.06; calculated ($C_{13}H_{10}NOBr$), C 56.55, H 3.65, N 5.07. IR (KBr) ν/cm^{-1}, 3415 (OH), 1638–1615 (C=N). ^{1}H-NMR ($CDC1_3$) δ/ppm, 5.10 (s, 1H, OH), 6.94 (d, 2H, Ar), 7.09 (d, 2H, Ar), 7.50 (d, 2H, Ar), 7.81 (d, 2H, Ar), 8.36 (s, 1H, CH=N).

Synthesis of Compound 2a

Compound **1a** (0.93 g, 4.0 mmole) was dissolved in 50 mL acetone in a round-bottom flask with the presence of potassium carbonate anhydrous (2.21 g, 16.0 mmole). 1,4-Dibromobutane (6.05 g, 28.0 mmole) was then added dropwise, and the mixture was subsequently refluxed for 18 h. The acetone solution was then left at room temperature to evaporate off. Fifty mL of water was subsequently added to the precipitate and the desired solid was filtered and dried. The product was recrystallized from chloroform. Yield 78%. Elemental analysis: found, C 55.70, H 4.68, N 3.83; calculated ($C_{17}H_{17}NOClBr$), C 55.68, H 4.67, N 3.82. IR (KBr) ν/cm^{-1}, 2940–2853 (C-H alkyl), 1608 (C=N), 1253 (O-CH_2). ^{1}H-NMR ($CDCl_3$) δ/ppm, 1.59–2.11 (m, 4H, CH_2), 3.54 (t, 2H, CH_2Br), 4.05 (t, 2H, OCH_2) 7.00 (d, 2H, Ar), 7.16 (d, 2H, Ar), 7.35 (d, 2H, Ar), 7.85 (d, 2H, Ar), 8.38 (s, 1H, CH=N).

Synthesis of Compound 2b

Yield 70%. Elemental analysis: found, C 57.82, H 5.36, N 3.56; calculated ($C_{19}H_{21}NOClBr$), C 57.84, H 5.36, N 3.55. IR (KBr) ν/cm^{-1}, 2935–2863 (C-H alkyl), 1607 (C=N), 1254 (O-CH2). ^{1}H-NMR ($CDCL_3$) δ/ppm, 1.53–1.95 (m, 8H, CH_2), 3.45 (t, 2H, CH_2Br), 4.05 (t, 2H, OCH_2), 7.00 (d, 2H, Ar), 7.16 (t, 2H, Ar), 7.34 (m, 2H, Ar), 7.83 (d, 2H, Ar), 8.37 (s, 1H, CH=N).

Synthesis of Compound 2c

Yield 80%. Elemental analysis: found, C 49.67, H 4.19, N 3.42; calculated ($C_{17}H_{17}NOBr_2$), C 49.66, H 4.17, N 3.41. IR (KBr) ν/cm^{-1}, 2943–2848 (C-H alkyl), 1622–1606 (C=N), 1252 (O-CH2). ^{1}H-NMR ($CDC1_3$) δ/ppm, 1.59–2.13 (m, 4H, CH_2), 3.53 (t, 2H, CH_2Br), 4.09 (t, 2H, OCH_2), 6.98 (d, 2H, Ar), 7.08 (d, 2H, Ar), 7.52 (d, 2H, Ar), 7.86 (d, 2H, Ar), 8.37 (s, 1H,CH=N).

Synthesis of Compound 2d

Yield 65%. E1emental analysis: found, C 51.98, H 4.84, N 3.20; calculated. ($C_{19}H_{21}NOBr_2$), C 51.96, H 4.82, N 3.19. IR (KBr) ν/cm^{-1}, 2940–2855 (C-H alkyl), 1618–1604 (C=N), 1248 (O-CH_2). ^{1}H-NMR ($CDCl_3$) δ/ppm, 1.53–1.95 (m, 8H, CH_2), 3.46 (t, 2H, CH_2Br), 4.05 (t, 2H, OCH_2), 7.00 (d, 2H, Ar), 7.10 (d, 2H, Ar), 7.52 (d, 2H, Ar), 7.83 (d, 2H, Ar), 8.36 (s, 1H, CH=N).

Synthesis of Compound 3a

In a round-bottom flask, compound **2a** (0.62 g, 1.7 mmole) and 2,4-dihydroxybenzaldehyde (0.11 g, 0.8 mmole) were dissolved in 50 mL of N,N′-dimethylformamide (DMF). Upon the addition of potassium carbonate anhydrous (0.44 g, 3.2 mmole), the mixture was heated at 70°C for 18 h and left to evaporate until 40 mL was left. The mixture was then cooled in ice bath for 0.5 h prior to addition of 50 mL of water. The precipitate was filtered off, dried, and recrystallized with hexane and chloroform mixture to yield the desired intermediate. Yield 61%. Elemental analysis: found, C 69,42, H 5.41, N 3.94; calculated ($C_{14}H_{38}N_2O,Cl_2$), C 69.39, H 5.40, N 3.95. IR (KBr) ν/cm^{-1}, 2949–2854 (C-H alkyl), 1670 (C=O), 1620–1605 (C=N), 1258 (O-CH_2). ^{1}H-NMR ($CDCl_3$) δ/ppm, 2.06 (m, 8H, CH_2), 4.14 (m, 8H, OCH_2), 6.46 (d, 1H, Ar), 6.58 (dd, 1H, Ar), 7.00 (dd, 4H, Ar), 7.16 (d, 4H, Ar), 7.35 (d, 4H, Ar), 7.84 (2d, 5H, Ar), 8.37 (s, 2H, CH=N), 10.36 (s, 1H, CH=O).

Synthesis of Compound 3b

Yield 63%. Elemental analysis: found, C 70.59, H 6.08, N 3.67; calculated ($C_{45}H_{46}N_2O_5Cl_2$), C 70.58, H 6.06, N 3.66. IR (KBr) ν/cm^{-1}, 2939–2853 (C-H alkyl), 1678 (C=O), 1620–1603 (C=N), 1254 (O-CH_2). ^{1}H-NMR ($CDC1_3$) δ/ppm, 1.57–1.89 (m, 16H, CH_2), 4.06 (m, 8H, OCH_2), 6.45 (d, 1H, Ar), 6.58 (dd, 1H, Ar), 7.00 (d, 4H, Ar), 7.16 (d, 4H, Ar), 7.35 (d, 4H, Ar), 7.83 (2d, 5H, Ar), 8.37 (s, 2H, CH=N), 10.35 (s, 1H, CH=O).

Synthesis of Compound 3c

Yield 56%. Elemental analysis: found, C 61.69, H 4.82, N 3.51; calculated ($C_{41}H_{38}N_2O_5Br_2$), C 61.67, H 4.80, N 3.51. IR (KBr) ν/cm^{-1}, 2951–2848 (C-H alkyl), 1670 (C=O) 1620–1606 (C=N), 1259 (O-CH_2). ^{1}H-NMR ($CDC1_3$) δ/ppm, 2.05 (m, 8H, CH_2), 4.14 (m, 8H, OCH_2), 6.45 (d, 1H, Ar), 6.58 (dd, 1H, Ar), 7.00 (dd, 4H, Ar), 7.10 (d, 4H, Ar), 7.49 (d, 4H, Ar), 7.84 (2d, 5H, Ar), 8.37 (s, 2H, CH=N), 10.36 (s, 1H, CH=O).

Synthesis of Compound 3d

Yield 58%. Elemental analysis: found, C 63.25, H 5.44, N 3.30; calculated ($C_{45}H_{46}N_2O_5Br_2$), C 63.24, H 5.42, N 3.28. IR (KBr) ν/cm^{-1}, 2940–2856 (C-H alkyl), 1676 (C=O), 1620–1603 (C=N), 1252 (O-CH_2). ^{1}H-NMR ($CDC1_3$) δ/ppm, 1.55–1.89 (m, 16H, CH_2), 4.06 (m, 8H, OCH_2), 6.45 (d, 1H, Ar), 6.56 (dd, 1H, Ar), 7.00 (d, 4H, Ar), 7.10 (d, 4H, Ar), 7.50 (d, 4H, Ar), 7.85 (2d, 5H, Ar), 8.36 (s, 2H, CH=N), 10.35 (s, 1H, CH=O).

Synthesis of Compound 4a

In a round-bottom flask, compound **3a** (0.28 g, 0.4 mmole) was dissolved in 7 mL of 4-ethylaniline. Forty mL absolute ethanol was then added to the stirring mixture and subsequently refluxed for 8 h. The mixture was then cooled in ice bath for 0.5 h. The resulting precipitate was filtered off and washed with hexane to remove the residue of 4-ethylaniline. The precipitate was re crystallized with hexane and chloroform mixture to yield the desired compound **4a**. Yield 61%. Elemental analysis: found, C 72.41, H 5.85, N 5.18; calculated ($C_{49}H_{47}N_3O_4Cl_2$), C 72.40, H 5.83, N 5.17. IR (KBr) ν/cm^{-1}, 2959–2872 (C-H alkyl), 1607–1594 (C=N), 1254 (O-CH_2). ^{1}H-NMR ($CDCl_3$) δ/ppm, 1.28 (t, 3H, CH_3), 1.61–2.05 (m, 8H, CH_2), 2.68 (q, 2H, CH_2), 4.13 (m, 8H, OCH_2), 6.48 (d, 1H, Ar), 6.61 (dd, 1H, Ar), 6.98 (2d, 4H, Ar), 7.16 (2d, 6H, Ar), 7.22 (2d, 6H, Ar), 7.85 (2d, 4H, Ar), 8.11 (d, 1H, Ar), 8.42 (2s, 2H, CH=N), 8.85 (s, 1H, CH=N).

Synthesis of Compound 4b

Yield 53%. Elemental analysis: found, C 73.28, H 6.40, N 4.85; calculated ($C_{53}H_{55}N_3O_4Cl_2$), C 73.26, H 6.38, N 4.84. IR (KBr) ν/cm^{-1}, 2941–2869 (C-H alkyl), 1623–1592 (C=N), 1249 (O-CH_2). ^{1}H-NMR ($CDC1_3$) δ/ppm, 1.28 (t, 3H, CH_3), 1.55–1.88 (m, 16H, CH_2), 2.70 (q, 2H, CH_2), 4.05 (m, 8H, OCH_2), 6.48 (d, 1H, Ar), 6.59 (dd, 1H, Ar), 6.98 (2d, 4H, Ar), 7.17 (2d, 6H, Ar), 7.22 (2d, 6H, Ar), 7.86 (2d, 4H, Ar), 8.12 (d, 1H, Ar), 8.41 (2s, 2H, CH=N), 8.85 (s, 1H, CH=N).

Synthesis of Compound 4c

Yield 50%. Elemental analysis: found, C 65.29, H 5.26, N 4.65; calculated ($C_{49}H_{47}N_3O_4Br_2$), C 65.27, H 5.25, N 4.66. IR (KBr) ν/cm^{-1}, 2959–2872 (C-H alkyl), 1607–1593 (C=N), 1254 (O-CH_2). ^{1}H-NMR ($CDC1_3$) δ/ppm, 1.28 (t, 3H, CH_3), 1.59–2.05 (m, 8H, CH_2), 2.68 (q, 2H, CH_2), 4.13 (m, 8H, OCH_2), 6.48 (d, 1H, Ar), 6.59 (dd, 1H, Ar), 6.98 (2d, 4H, Ar), 7.17 (2d, 6H, Ar), 7.22 (2d, 6H, Ar), 7.84 (2d, 4H, Ar), 8.11 (d, 1H, Ar), 8.40 (2s, 2H, CH=N), 8.85 (s, 1H, CH=N).

Synthesis of Compound 4d

Yield 56%. Elemental analysis: found, C 66.47, H 5.81, N 4.41; calculated ($C_{53}H_{55}N_3O_4Br_2$), C 66.46, H 5.79, N 4.39. IR (KBr) ν/cm^{-1}, 2941–2870 (C-H alkyl), 1624–1592 (C=N), 1251 (O-CH_2). ^{1}H-NMR ($CDCl_3$) δ/ppm, 1.27 (t, 3H, CH_3), 1.56–1.88 (m, 16H, CH_2), 2.68 (q, 2H, CH_2), 4.05 (m, 8H, OCH_2), 6.48 (d, 1H, Ar), 6.59 (dd, 1H, Ar), 6.98 (2d, 4H, Ar), 7.17 (2d, 6H, Ar), 7.22 (2d, 6H, Ar), 7.84 (2d, 4H, Ar), 8.09 (d, 1H, Ar), 8.41 (2s, 2H, CH=N), 8.85 (s, 1H, CH=N).

Synthesis of Compound 5a

The method to synthesize compound **5a** and the rest of the fluorinated homologs is similar to the synthesis of **4a** of which 4-ethylaniline was substituted by 4-fluoroaniline. Yield 57%. Elemental analysis: found, C 70.34, H 5.28, N 5.25; calculated ($C_{47}H_{42}N_3O_4FCl_2$), C 70.32, H 5.27, N 5.23. IR (KBr) ν/cm^{-1}, 2957–2877 (C-H alkyl), 1626–1594 (C=N), 1251 (O-CH_2). ^{1}H-NMR ($CDCL_3$) δ/ppm, 2.05 (m, 8H, CH_2), 4.13 (m, 8H, OCH_2), 6.49 (d, 1H, Ar), 6.59 (dd, 1H, Ar), 6.99 (2d, 4H, Ar), 7.09 (m, 6H, Ar), 7.19 (m, 6H, Ar), 7.81 (2d, 4H, Ar), 8.10 (d, 1H, Ar), 8.38 (2s, 2H, CH=N), 8.81 (s, 1H, CH=N).

Synthesis of Compound 5b

"Yield 60%. Elemental analysis: found, C 71.33, H 5.87, N 4.90; calculated ($C_{5l}H_{50}N_3O_4FCl_2$), C 71.32, H 5.87, N 4.89. IR (KBr) ν/cm^{-1}, 2944–2870 (C-H alkyl), 1623–1593 (C=N), 1251 (O-CH_2). ^{1}H-NMR ($CDCl_3$) δ/ppm, 1.58–1.89 (m, 16H, CH_2), 4.06 (m, 8H, OCH_2), 6.48 (d, 1H, Ar), 6.59 (dd, 1H, Ar), 6.98 (2d, 4H, Ar), 7.08 (m, 6H, Ar), 7.17 (m, 6H, Ar), 7.83 (2d, 4H, Ar), 8.08 (d, 1H, Ar), 8.38 (2s, 2H, CH=N), 8.81 (s, 1H, CH=N).

Synthesis of Compound 5c

Yield 50%. Elemental analysis: found, C 63.33, H 4.76, N 4.72; calculated ($C_{47}H_{42}N_3O_4FBr_2$), C 63.31, H 4.75, N 4.71. IR (KBr) ν/cm^{-1}, 2958–2877 (C-H alkyl), 1626–1594 (C=N), 1251 (O-CH_2). ^{1}H-NMR

($CDC1_3$) δ/ppm, 2.06 (m, 8H, CH_2), 4.13 (m, 8H, OCH_2), 6.49 (d, 1H, Ar), 6.59 (dd, 1H, Ar), 7.01 (2d, 4H, Ar), 7.09 (m, 6H Ar), 7.19 (m, 6H, Ar), 7.84 (2d, 4H, Ar), 8.09 (d, 1H, Ar), 8.39 (2s, 2H, CH=N), 8.81 (s, 1H, CH=N).

Synthesis of Compound 5d

Yield 67%. Elemental analysis: found, C 64.65, H 5.34, N 4.43; calculated ($C_{51}H_{50}O_4FBr_2$), C 64.63, H 5.32, N_3 N 4.43. IR (KBr) ν/cm^{-1}, 2946–2873 (C-H alkyl), 1623–1594 (C=N), 1252 (O-CH_2). ^{1}H-NMR ($CDCl_3$) δ/ppm, 1.55–1.89 (m, 16H, CH_2), 4.06 (m, 8H, OCH_2), 6.48 (d, 1H, Ar), 6.59 (dd, 1H, Ar), 6.98 (2d, 4H, Ar), 7.09 (m, 6H, Ar), 7.18 (m, 6H, Ar), 7.83 (2d, 4H, Ar), 8.08 (d, 1H, Ar), 8.38 (2s, 2H, CH=N), 8.81 (s, 1H, CH=N).

Characterization

Elucidation of molecular structure of intermediary and title compounds was obtained by FT-IR and ^{1}H-NMR spectroscopy. The FT-IR spectroscopy was performed on a Perkin Elmer 2000 FTIR spectrometer. The samples were prepared in KBr pellets and the spectra were recorded within 4000-400 cm^{-1}. The ^{1}H-NMR spectroscopy was carried out on a Bruker 400 MHz Ultrashield^{TM} spectrometer. Deuterated chloroform ($CDCl_3$) with TMS as internal standard was used to dissolve 20 mg of samples in the NMR tube. For compounds **1a** and **1b**, the temperature was maintained at 50°C using the spectrometer internal heater throughout the analyses. CHN microanalyses were conducted via Perkin Elmer 2400 LS Series CHNS/O analyzer. The optical properties of the compounds were investigated using a Carl Zeiss Axioskop 40 polarizing microscope linked to a Linkam TMS94 temperature controller and LTS350 hot-stage. Differential scanning calorimetry was performed on a Seiko DSC6200R calorimeter with the heating and cooling rate of $\pm 5°Cmin^{-1}$ at Tokyo Institute of Technology, Japan. Powder X-ray diffraction analysis on a representative compound **4c** was conducted using a Bruker D8 diffractometer at Warsaw University, Poland. On the same sample, further conformational studies were carried out based on MM2 calculations with minimum energetic parameters. The software used for the calculations is CS Chem3D Pro produced by CambridgeSoft Corporation.

RESULTS AND DISCUSSION

Thermal and Liquid Crystalline Properties

The phase sequences, transition temperatures, and associated enthalpies for compounds **3a–3d**, **4a–4d**, and **5a–5d** are collated in Table 2.

TABLE 2 Phase Transition Temperatures (°C) and Associated Enthalpies (kJ mol^{-1}) of Compounds **3a–3d**, **4a–4d**, and **5a–5d** (● = enantiotropic phase, ○ = monotropic phase, only the Highest Melting Point of Crystal is Reported. T_g = glass transition temperature, Cr = crystal, N = nematic, I = isotropic)

Compound	T_g	Cr		N		I
3a		●	132.7 (30.6)	○	[122.2][a]	●
3b		●	100.1 (25.2)	●	106.2 (1.4)	●
3c		●	125.3 (19.0)			●
3d		●	111.4 (41.3)	○	[98.5] (4.1)	●
4a	13.4 (0.4)[b]	●	117.6 (54.5)	●	144.3 (4.7)	●
4b	5.2 (0.3)[b]	●	138.0 (81.9)	○	[117.7] (3.9)	●
4c		●	119.8 (29.5)	●	146.5 (5.3)	●
4d		●	133.1 (95.1)	○	[119.0] (5.9)	●
5a		●	155.2 (73.5)	○	[141.6] (4.0)	●
5b		●	130.1 (77.6)	○	[124.5] (5.1)	●
5c		●	156.5 (86.7)	○	[143.2] (5.0)	●
5d		●	137.3 (29.3)	○	[117.2] (4.0)	●

[] Denotes transition temperature in formation of monotropic N phase.

[a] Denotes transition temperature by polarizing microscopy, undetectable by DSC.

[b] Denotes heat capacity change in kJ $(mol \cdot °C)^{-1}$ accompanying glass transition directly to N phase from 2nd heating run onwards; pure Cr phase is only observed for the 1st heating run.

Representative DSC traces of compounds **4a** and **4b** are depicted in Fig. 1a and 1b, respectively. Compound **3a** exhibits monotropic nematic phase. By increasing the spacer length from C_4H_8 to C_6H_{12},the enantiotropic nematic phase is observed for compound **3b**. On the other hand, compound **3c** is not mesogenic. However, the monotropic nematogenic properties of the Br homolog are induced by replacing C_4H_8 with C_6H_{12} spacers for compound **3d.** The overall phase transitions for compounds **3a–3d** as depicted in Fig. 2 indicate that the compounds **3b** and **3d** with C_6H_{12} members possess greater tendency in comparison to C_4H_8 members (**3a** and **3c**) in exhibiting nematic phase. This observation could possibly be due to the increase in molecular flexibility in compounds **3b** and **3d** leading to the reduction of strong intermolecular forces induced at the aldehyde core.

With the presence of 4-ethylaniline fragment, both chlorinated and brominated trimers exhibit nematogenic properties. However, the mesomorphic properties of compounds **4a–4d** are in contrast to the results we obtained for **3a–3d** as discussed earlier. The compounds **4a** and **4c** consisting C_4H_8 members exhibit enantiotropic nematic phase. By increasing the spacer length to C_6H_{12}, the monotropic nematic phase was detected for compounds **4b** and **4d**. The presence

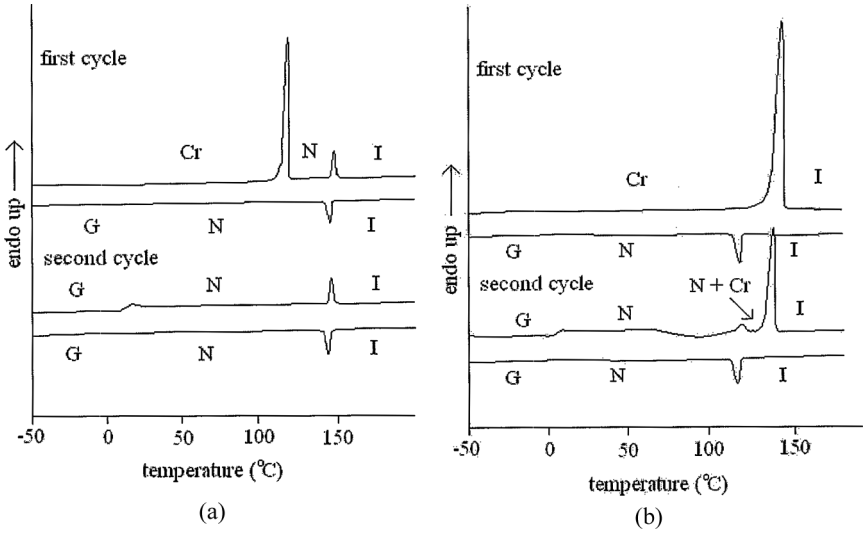

FIGURE 1 DSC traces of (a) compound **4a** with heat capacity change of 0.4 kJ (mol·°C)$^{-1}$ at 13.4°C and (b) compound **4b** with heat capacity change of 0.3 kJ (mol·°C)$^{-1}$ at 5.2°C. G indicates the glassy state. The heat capacity change is observed at G-N phase transition upon second heating.

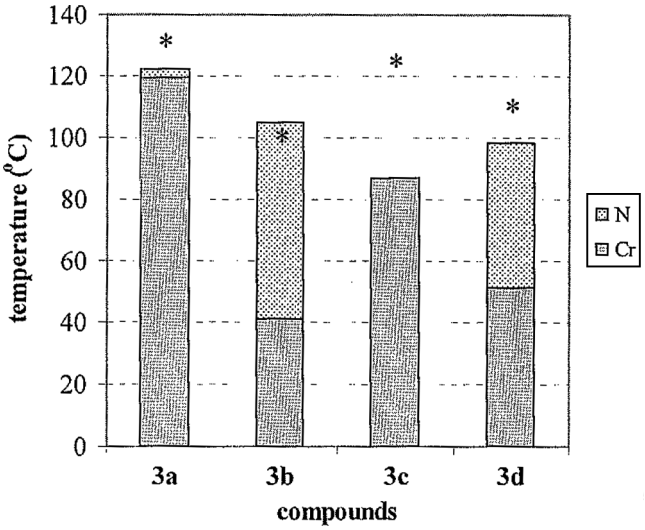

FIGURE 2 The plot of phase temperature (°C) range upon cooling for compounds **3a–3d** (* denotes mp).

of enantiotropic nematic phase for the butyl members suggests the higher phase stability in comparison to the hexyl members. Although compounds **4a** and **4c** possess relatively short flexible spacers, the flexibility of the molecule as a whole is sufficient to stabilize the nematic phase due to the presence of an additional ethyl group at the central core. The additional two methylene units in **4b** and **4d** results in excess of flexibility which hinder the formation of enantiotropic nematic phase.

By introducing a polar fluorine atom to the central mesogenic core, all trimers exhibit monotropic nematic phase. The monotropic nematic temperature ranges of compounds **5a–5d** are shown in Fig. 3 based on DSC result with heating and cooling rate of $\pm 5^{\circ}\mathrm{C min}^{-1}$. As previously reported on fluorinated derivatives with various mesogenie cores, the fluorine atom is known to alter the thermal and chemical stability and viscosity of liquid crystals [11]. For compounds **5a–5d**, introduction of a polar fluorine atom increases the polarity at the middle segment of the trimeric structure. As such, the terminal attractions of the trimers will be affected causing the decrease in the stability of the nematic phase. This observation contradicts with those compounds having higher degree of terminal intermolecular attractions which favors the formation of nematic phase [12]. For compounds **5a–5d**, even with

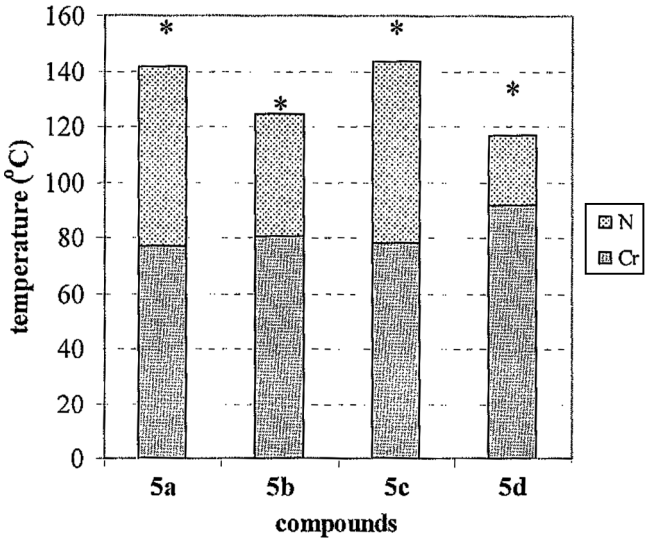

FIGURE 3 The plot of phase temperature (°C) range upon cooling for fluorinated compounds **5a–5d** (* denotes mp).

a polar fluorine atom the smectic phase could not be induced. The layered arrangement in the smectic phase is not possible because of the branched structure of the trimers and lower degree of shape anisotropy as reported for a series of azobenzene derivatives with lateral alkoxy group [13].

Among the twelve homologous members, full recrystallization from the nematic phase upon cooling is not observed for compounds **4a–4c**. Instead, the microscopic samples undergo the glass transition at low temperatures like a polymer and therefore exhibit the glassy state. This characteristic is evident by the observation of noncrystalline texture which closely resembles the nematic schlieren texture on supercooling below room temperature. In such a condition, the orientational order characteristic of the nematogenic fluid is frozen in the solid state [14]. The melting point of compound **4a** (117.6°C) can only be detected on first heating in which the latent heat of fusion is 54.5 kJ mol^{-1}. Under polarized light, it is observed that the cooling of the sample increases the viscosity but no Cr phase is visually detected. Our observation is, however, consistent with the DSC result as N-Cr transition is absent even when sample is cooled to −40°C (Fig. 1a). On second heating, instead of the melting point, the glass transition is detected by DSC at 13.4°C with heat capacity change of 0.4 kJ $(mol \cdot °C^{-1})$.

Compound **4b** exhibits similar glassy texture of compound **4a**. However, there are two important differences between the two homologs. On first heating, in contrast to compound **4a**, the nematic phase is not observed for compound **4b**. The second notable difference is the presence of a broad exothermic curve between 67.0°C and 118.0°C on heating of compound **4b** as shown in the DSC trace (Fig. 1b). This signal indicates the occurrence of some recrystallization at the same time heat is consistently applied to the sample at $5°Cmin^{-1}$. At 118.8°C, a small endothermic peak (0.8 kJ mol^{-1}) is assigned to slight melting transition. Upon further heating, the sample clears into isotropic at 137.4°C with an enthalpy value of 51.5 kJ mol^{-1}. This high isotropization enthalpy indicates that the melting involves crystalline structure and certainly not only the nematic phase despite that schlieren texture is clearly observed.

Similar to compound **4a**, compound **4c** is an enantiotropic nematogen. On second heating, a step change which represents heat capacity change is not observed in the DSC thermogram as expected. On the other hand, an endothermic peak with $1.0\,kJ\,mol^{-1}$ is detected at 14.6°C. This peak indicates some recrystallization over the glassy state prior to this transition. At 119.9°C, a peak measuring 0.9 kJ mol^{-1} is detected by DSC. This temperature is consistent with the melting

temperature (119.8°C) upon first heating and, therefore, suggests that minor recrystallization occurs in the nematic matrix before 119.9°C upon second heating. The low enthalpy (0.9 kJ mol^{-1}) indicates that the major portion of the sample is in the nematic phase despite the occurrence of some recrystallization. In terms of textural observation, both nematic and crystal phases are not detectable under polarized light as nematic schlieren texture covers the whole microscopic domain.

Compound **4d** exhibits monotropic nematic phase. Unlike compounds **4a–4c**, the glassy state is not observed for compound **4d**. Recrystallization of the sample upon cooling is evident under the polarized light for both first and second cycles and the observation is in agreement with the DSC results as N-Cr transition is detected thermodynamically.

In order to further investigate the nematic phase and glassy state, powder X-ray diffraction was conducted on representative compound **4c**. The X-ray diffraction intensity profile of the nematic phase is given in Fig. 4. The peak position corresponds to 32 Å in terms of average distances among molecules and the peak broadness indicates the short range positional order in the nematic phase. It is also observed that the shape of the signal fits the Lorentzian function as typically obtained for phases with short range order. From MM2 calculations, the proposed most stable conformation of **4c** trimer is approximately 40 Å measuring from one Br-substituted terminal to another end as

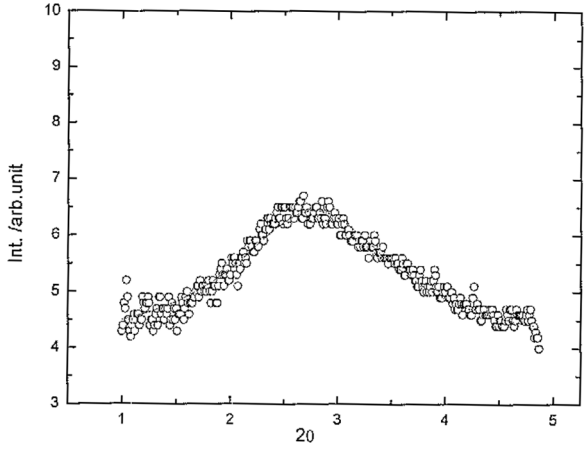

FIGURE 4 The powder X-ray diffraction intensity profile for compound **4c** in the nematic phase (120.0°C) The red line indicates that the signal fits the Lorentzian function.

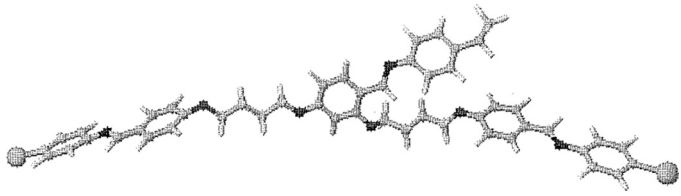

FIGURE 5 Proposed conformation of **4c** based on MM2 calculations with minimum energetic parameters. The conformation measures approximately 40 Å.

shown in Fig. 5. The d/l value of 0.8 suggests some intercalation among the trimers in the nematic phase which is not uncommon. On the other hand, the glassy state of compound **4c** could not be analyzed via powder X-ray diffraction as the state only exists below 14.6°C. However, because the glassy state and the nematic phase are similar in terms of orders, the positional order in the glassy state is extrapolated from the powder X-ray diffraction results obtained for the nematic phase.

The low glass transition temperatures of compounds **4a–4c** are attributable to the flexibility induced by the mefhylene spacers and most importantly, the ethyl group at the central core [15]. This explanation is further supported by the ability of compounds **5a–5d** which do not have an ethyl group, to recrystallize despite possessing recrystallization temperature more than 40°C below the melting point.

Although most substituents at lateral position are known to create some hindrance, the small size of a fluorine atom minimizes such effect in comparison to bulkier groups such as the ethyl chain. From DSC and polarizing microscopy, we found that the microscopic samples of **5a–5d** are able to recrystallize to the original crystal phase upon cooling of the nematic phase. This characteristic suggests that the fluorinated trimers have less difficulty to pack into the crystal lattices from the nematic phase.

From the microscopic observation, all mesogenic trimers in this series exhibit schlieren texture with twofold ($s = \pm 1/2$) and fourfold ($s = \pm 1$) brushes as depicted in Fig. 6. The schlieren texture indicates that the director is parallel to the untreated glass supports and. varies slowly in the planes [16]. On the other hand, the thin preparation of compound **4c** between the substrates gives rise to marble texture instead of the schlieren texture.

The T_{NI} of compound **4a** is higher than the T_m of compound **4b** which exhibits monotropic nematic phase. Similar characteristics

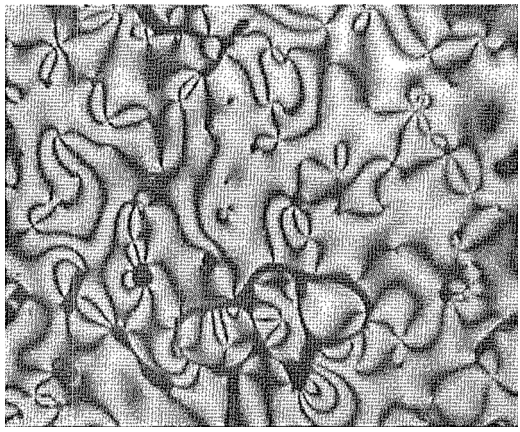

FIGURE 6 The texture of schileren defect with twofold and fourfold brushes of compound **4d** 117.8°C on cooling.

are also observed for compounds **4c** and **4d**. For compounds **5a–5d**, the trimers with C_4H_8 spacers possess higher T_m than the corresoponding homologues with C_6H_{12} spacers. The lowering of T_m or T_c with the increase of spacer length indicates dilution of the mesogenic cores as reported for other series of trimeric liquid crystals such as 4,4′-bis[ω-(4-cyanobiphenyl-4′-yloxy)alkoxy]biphenyls [17].

The transition temperatures (T_m and T_c) recorded for the twelve trimers are lower than 160°C. Generally, for trimeric structure, the presence of three mesogenic cores often gives rise to higher transition temperatures. In this series of nonsymmetric trimers, the relatively low transition temperatures can be attributed to the branched molecular architecture at the central core.

The exclusive nematogenic characteristics of the trimers can also be explained from the viewpoint of trimeric structure. The lower shape anisotropy of the trimers due to branching at the 2,4-dihydroxybenzaldehyde aromatic ring results in less ordered mesophase. The addition of another aromatic ring to the central core increases the overall transition temperatures of the trimers as reported in the homologous series of 4-(trans-4′-*n*-pentylcyclohexyl) benzoates [18]. Compounds **3c**, **4c**, and **5c**, n particular, exhibit three different types of thermal properties with respect to the changes in the central mesogenic fragment. From being non-mesogenic for compound **3c**, enantiotropic nematic phase is induced for **4c** with addition of 4-ethylaniline fragment. By substituting the ethyl group with a fluorine atom, the monotropic nematic phase is observed for **5c**.

CONCLUSIONS

Series of nonsymmetric 4-ethyl- and 4-fluoroanilinebenzylidene-2′,4′-oxy-bis(4″-halogenoanilinebenzylidene-4‴-oxy)alkanes trimers have been synthesized and characterized, for their liquid crystalline properties. The trimers differ from each other in terms of C_4H_8 or C_6H_{12} flexible spacers, terminal X of Cl or Br atom, and terminal Y of F atom or C_2H_5 group. Every member in this series was nematogenic. Enantiotropic nematic phase was observed only for the trimers with C_2H_5 group and C_4H_8 spacer. For compounds **4a–4d**, lengthening the $C_4$4H_8 spacer to C_6H_{12} led to the monotropic nature of the nematic phase. Compounds **4a–4c** exhibited the glassy nematic state as the molecular motion in the nematic phase was frozen on cooling. The T_g for compounds **4a** and **4b** were detected below 15°C by DSC. For compound **4c**, instead of a step change in heat capacity, a peak which indicates an enthalpy was observed in the DSC thermogram. The glassy state of the compounds **4a–4c** can be attributed to the presence of the C_2H_5 group because such property was not observed for the fluorinated trimers. In contrast to C_2H_5 homologues, all F-substituted trimers **5a–5d** recrystallized on cooling the nematic phase. The fluorinated homologues exhibited monotropic nematic phase regardless of spacers and terminal halogen atoms.

ACKNOWLEDGMENTS

The main author (G.-Y. Yeap) would like to thank the Malaysian Ministry of Science, Technology, and Innovation (MOSTI) and Ministry of Higher Education for providing financial support via Science Fund (03-01-05-SF0062 or 305/PKIMIA/613315) and Fundamental Research Grant Scheme (304/PKIMIA/671025), respectively. Authors are also grateful to the Research and Innovation Division in Universiti Sains Malaysia for the support and assistance.

REFERENCES

[1] Imrie, C. T. & Henderson, P. A. (2002). *Cur. Op. Coll. Int. Sc.*, *7*, 298.
[2] Yoshizawa, A., Kinbara, H., Narumi, T., Yamaguchi, A. & Dewa, H. (2005). *Liq.Cryst.*, *32*, 1175.
[3] Imrie, C. T. & Luckhurst, G. R. (2001). *J. Mater. Chem.*, *8*, 1339.
[4] Yelamaggad, C. V., Nagamani, S. A., Hiremath, U. S. , Rao, D. S. S., & Prasad, S. K. (2001). *Liq. Cryst.*, *28*, 1581.
[5] Attard, G. S., Date, R. W., Imrie, C. T., Luckluirst, G. R., Roskilly, S. J., Seddon, J. M., & Taylor, L. (1994). *Liq. Cryst.*, *16*, 529.
[6] Blatch, A. E., Fletcher, I. D., & Luckhurst, G. R. (1995). *Liq. Cryst.*, *18*, 801.

[7] Tschierske, C. (2001). *J. Mater. Chem.*, *11*, 2647.
[8] Mori, A., Kubo, K., Takemoto, M., & Ujiie, S. (2005). *Liq. Cryst.*, *32*, 1021.
[9] Belmar, J., Parra, M., Zuniga, C., Perez, C., Muftoz, C., Omenat, A., & Serrano, J. L. (1999). *Liq. Cryst.*, *26*, 389.
[10] Berdague, P., Bayle, J. P., Ho, M. S., & Fung, B. M. (1993). *Liq. Cryst.*, *14*, 667.
[11] Pavluchenko, A. I., Smimova, N. I., Petrov, V. F., Fialkov, Y. A., Shelyazhenko, S. V., & Yagupolsky, L. M. (1991). *Mol. Cryst Liq. Cryst.*, *209*, 225.
[12] Cerrada, P., Marcos, M., & Serrano, J. L. (1989). *Mol. Cryst. Liq. Cryst.*, *170*, 79.
[13] Prajapati, A. K., Vora, R. A., & Pandya, H. M. (2001). *Mol. Cryst. Liq. Cryst.*, *369*, 37.
[14] Fan, F. Y., Culligan, S. W., Mastrangelo, J. C., Katsis, D., Chen, S. H., & Blanton, T. N. (2001). *Chem. Mater.*, *13*, 4584.
[15] Zhao, W., KLoczkowski, A., Mark, J. E., Erman, B., & Bahar, I. (1996). *Macromolcules*, *29*, 2796.
[16] Dierking, I. (2003). *Textures of Liquid Crystals.*, Wiley-VCH: Weinheim, Germany.
[17] Imrie, C. T., & Luckhurst, G. R. (1998). *J. Mater. Chem.*, *8*, 1339.
[18] Dabrowski, R., Dziaduszek, J., Szczucinski, T., & Raszewski, Z. (1984). *Mol. Cryst. Liq. Cryst.*, *107*, 411.
[19] So, B. K., Kim, W. J., Lee, S. M., Jang, M. C., Song, H. H., & Park, J. H. (2007). *Dyes Pigments*, *75*, 619,
[20] Balsells, J., Mejorado, L., Phillips, M., Ortega, F., Aguirre, G. Somanathan, R., & Walsh, P. J. (1998). *Tetrahedron: Asym.*, *9*, 4135.